Improved Artificial Hummingbird Algorithm for Optimal Allocation of SVCs in Distribution Networks to Maximize Energy Efficiency

Ali S. Aljumah, *Member*, *IEEE*, Mohammed H. Alqahtani, *Member*, *IEEE,* Ahmed R. Ginidi, and Abdullah M. Shaheen

***Abstract*—The static var compensator (SVC) is a cost-effective device in flexible AC transmission system (FACTS) family. We introduce an improved artificial hummingbird algorithm (IAHA) for optimal allocation of SVCs in distribution networks to maximize energy efficiency. Three loading levels (low, medium, and high) per day are investigated. The proposed IAHA is evaluated on the IEEE 33-bus distribution network (DN) and 69-bus DN. The proposed IAHA demonstrates notable improvements in cost savings and voltage profile compared with the conventional artificial hummingbird algorithm (AHA). In addition, it enhances energy savings across various loading conditions and outperforms the conventional AHA in both best and average performance metrics. Although raising the compensation limit initially increases cost savings, the benefits decrease beyond a threshold, highlighting the importance of balancing the compensation levels for maximum efficiency.**

***Index Terms*—Improved artificial hummingbird algorithm (IAHA), distribution network (DN), flexible AC transmission system (FACTS), static var compensator (SVC), energy efficiency.**

I. Introduction

DISTRIBUTION networks (DNs) have recently attracted the interest of researchers owing to their critical role in power system quality and planning. Losses are relatively high in DNs that operate at low voltages and high currents. Various approaches have been investigated to reduce losses, including distributed generator (DG) placement [1], [2], system topology reconfiguration [3], and reactive power compensation [4], [5]. DG placement in DN is an efficient method for reducing system losses. Furthermore, loss minimization in DN is investigated by applying a modified success-history-based adaptive differential evolution (DE) algorithm to determine the best values for the outputs of rescheduling generators in addition to DG source placement/sizing based on locational marginal pricing [6]. System topology reconfiguration, commonly referred to as network reconfiguration, can be applied through changes in line connection, where two types of switches are designed in primary DNs [7], [8]. Tie switches are often normally opened and placed first, followed by normally closed sectionalizing switches. These switches enable configurability and provide protection. The system topology can be modified by changing the statuses of these switches (opened/closed) while maintaining the DN radiality constraint [9]. In [10], a bi-level optimization method is achieved using a particle swarm optimizer for coordinated reconfiguration and expansion planning with demand response activation. Despite the enhanced effectiveness of the method proposed in [10], its performance is validated using a small standard IEEE 33-bus DN.

Many reactive power compensators are used to reduce system losses. These compensators should be optimally allocated to maximize their effect. Shunt capacitors (SCs) and static var compensators (SVCs) are powerful components in reactive power compensators. In [11], SCs are optimally allocated using a sine-cosine optimizer. The objective function aims to enhance the reliability and reduce system losses through two strategies. First, a loss sensitivity factor is allowed to find the best locations for SC installation. Second, a sine-cosine optimizer is used to determine the optimal SC rating. Hourly load variations are also considered. In [12], SVC and thyristor-controlled series capacitor are included in the reactive power dispatch and handled using a refined lightning-attaching optimizer. In [12], the traditional lightning-attaching optimizer is refined by integrating spiral orientation motion and Lévy flight distribution to reduce system losses, voltage fluctuations, and overall operational costs. In addition to the SVC and thyristor-controlled series capacitor, a static synchronous compensator is proposed based on the artificial bee colony in [13] to reduce transmission line losses. In [14], a multi-objective antlion optimization technique is presented to determine the optimal placement and sizing of DGs in a DN. The technique in [14] mimics the foraging

Manuscript received: December 25, 2024; revised: February 21, 2025; accepted: April 14, 2025. Date of CrossCheck: April 14, 2025. Date of online publication: June 13, 2025.

The authors extend their appreciation to Prince Sattam bin Abdulaziz University for funding this research work through the project number PSAU/2024/01/31685.

A. S. Aljumah and M. H. Alqahtani are with the Department of Electrical Engineering, College of Engineering, Prince Sattam bin Abdulaziz University, Al Kharj, Saudi Arabia (e-mail: as.aljumah@psau.edu.sa; mh.alqahtani@psau.edu.sa).

A. R. Ginidi and A. M. Shaheen (corresponding author) are with the Electrical Engineering Department, Faculty of Engineering, Suez University, Suez, Egypt (e-mail: ahmed.ginidi@eng.suezuni.edu.eg; abdullahshaheen2015@gmail.com).

DOI: 10.35833/MPCE.2024.001380

behavior of antlions through five key phases: random position adjustment, trap construction, ant trapping, prey capture, and trap reconstruction. Multi-objective antlion optimization technique is applied to minimize system losses, support voltage stability, and maintain balanced loads while addressing load imbalances and excessive voltage increases at buses containing DGs. However, multi-objective antlion optimization technique is designed for and applied to the small-scale DN, particularly the IEEE 33-bus radial DN. In [15], the best positions for SVCs are determined using particle swarm optimization, which is subsequently used to establish the dispatch strategy. This particle swarm optimization is aimed to maximize the cost savings while considering limits in voltage and total harmonic distortion. In [16], SVCs are developed to regulate nodal voltage variations under irregular wind and solar power generation. Despite successful application and improved performance in practical case studies in the Banat region of Serbia, only a small-scale DN is evaluated. In [17], SVC positioning is intended to increase the static voltage stability using the *L*-index. However, the method in [17] is tested on a sample radial DN and 24-bus equivalent high-voltage DN. In [18], a single SVC is placed and installed with specified sizes of 5, 15, 25, 35, and 35 Mvar in the IEEE 9-bus DN and 30-bus DN to support their voltage profiles and minimize system losses. In [19], bald eagle search is applied to allocate DGs coordinated with SCs in DNs to minimize power losses. However, only baseline loading is evaluated in [18] and [19].

In [20], hybrid cuckoo search and antlion optimization are applied to allocate 12 SVCs to an IEEE 57-bus DN. Reference [20] considers branch outages of lines 50 and 41 as the worst-case scenarios. However, the allocation and sizing of the SVCs vary significantly across various outage scenarios, making it impractical for real-world applications. In [21], SVCs and static synchronous compensators are optimally placed in an IEEE 14-bus DN to regulate the bus voltage levels. In addition, a ranking method based on three voltage drop indices is introduced to determine the optimal installation location in [21]. However, this method is constrained to the installation of a single SVC, and its effectiveness is validated using a small test system, likely limiting its scalability. In [22], a guided surrogate gradient-based evolutionary strategy is designed for SVC to mitigate interarea oscillations in power systems. This strategy trains a reinforcement learning agent to determine the optimal SVC control strategies, ensuring fast oscillation damping. In [23], mayfly optimization, firefly algorithm, and particle swarm optimization are applied to optimize the controller parameters of the SVC and power system stabilizer, improving the system stability in a multimachine power network. In [24], a gradient-based optimizer (GBO) is utilized for SVC allocation in DNs to minimize system losses. However, it neglects the hourly load variations, which is crucial for real-time power system operation. In [25], a modified enhanced moth flame optimization algorithm is proposed to determine the optimal position and sizing of SVC and thyristor-controlled series capacitor in an IEEE 57-bus DN. Although the system losses are reduced and power system loading ability is improved using continuous power flow under both equality and inequality constraints, optimization is conducted solely under peak load conditions, limiting its applicability to real-world dynamic loading scenarios.

The conventional artificial hummingbird algorithm (AHA) [26] emulates the flying ability and foraging behaviors of hummingbirds. Foraging patterns involving axial, diagonal, and omnidirectional movements are used. In addition, a visit table is constructed to simulate the bird search for food. All hummingbird agents in AHA have certain food sources that they can use for survival. In addition, a hummingbird agent can recall the location and frequency of nectar replenishment at every foraging location [27]. Moreover, it can track the period during which a food source has been exploited without being examined [28]. The AHA has achieved remarkable performance and versatility, quickly attracting research interest. Furthermore, several implementations of AHA have been investigated in various domains, including microgrid energy management systems [29], Internet of Things, forecasting, feature selection, clustering, classification, scheduling, image processing, wireless sensor networks, and other engineering areas [30], [31].

We introduce an improved AHA (IAHA) with a regulated foraging pattern to optimize allocation of SVC in DNs and maximize annual energy savings, focusing on loading variation control. Although previous research has explored the optimal placement of reactive power compensators using heuristic techniques, many studies have either focused on small networks or lacked adaptive allocation strategies for varying load conditions. Additionally, existing studies on SVC deployment have not fully investigated the impact of compensation limits on cost savings and voltage profile.

This study bridges current research gaps by providing key contributions as follows.

1) Proposing a time-dependent operational allocation of SVCs in DNs to enhance adaptability across various loading conditions.

2) Introducing an IAHA with enhanced exploration balance, thus achieving improvement in cost savings.

3) Incorporating varying compensation limits as supplementary constraints for the overall reactive power demand.

4) Providing a detailed economic and technical analysis to optimize financial and operational performance.

5) Validating the superiority of the proposed IAHA over similar algorithms such as DE algorithm [32], dwarf mongoose optimization algorithm (DMOA) [33], salp swarm algorithm (SSA) [34], [35], GBO [36], and honey badger algorithm (HBA) [37].

II. Time-dependent Operational Allocation of SVCs in DNs

We propose a time-dependent operational allocation of SVCs in DNs, in which different loading levels are considered. The corresponding model (SVC model) considers SVC controllability because each device is described as either a negative or positive supply of the reactive power. Therefore, the SVC outputs are managed and adapted every hour to obtain operational benefits. The cost savings related to the energy losses *OV* are considered as the objective function, which is given as:

$$OV = K_e \sum_{LV=1}^{N_{LV}} (P_{Losses_0} - P_{Losses_A}) \cdot Interval_{LV} \quad (1)$$

where K_e is the cost, which is expressed in \$/kWh; P_{Losses_0} is the initial power loss; P_{Losses_A} is the power loss after optimal sizing, placing, and operation of the SVCs by the proposed IAHA; $Interval_{LV}$ is the time interval in hour at loading level LV, $LV \in [1, 24]$; and N_{LV} is the number of loading levels.

For allocation of SVC, decision variables are categorized into three groups: ① installed bus locations; ② reactive power capacity of each installed device; and ③ output of each installed device at different loading levels. These decision variables collectively form vector $\boldsymbol{CV}$, which is optimized using the proposed IAHA. According to the proposed time-dependent operational allocation of SVCs, the vector of decision variables can be mathematically modeled as:

$$\boldsymbol{CV}^{\mathrm{T}} = \begin{bmatrix} bus_1, bus_2, \ldots, bus_{N_{svc}} \\ Qsvc_{bus_1}^{Rate}, Qsvc_{bus_2}^{Rate}, \ldots, Qsvc_{bus_{N_{svc}}}^{Rate} \\ Qsvc_{bus_1,1}, Qsvc_{bus_2,1}, \ldots, Qsvc_{bus_{N_{svc}},1} \\ Qsvc_{bus_1,2}, Qsvc_{bus_2,2}, \ldots, Qsvc_{bus_{N_{svc}},2} \\ \vdots \\ Qsvc_{bus_1,N_{LV}}, Qsvc_{bus_2,N_{LV}}, \ldots, Qsvc_{bus_{N_{svc}},N_{LV}} \end{bmatrix} \quad (2)$$

where subscript N_{svc} is the number of installed SVCs; bus_I ($I = 1, 2, \ldots, N_{svc}$) is the candidate bus I to install SVC; $Qsvc_{bus_I}^{Rate}$ is the rated SVC capacity at bus I; and $Qsvc_{bus_I,LV}$ ($LV = 1, 2, \ldots, N_{LV}$) is the SVC capacity at bus I at loading level LV.

The total number of decision variables is $N_{svc} + N_{svc} + N_{svc}N_{LV}$. For instance, if three SVCs (i. e., $N_{svc} = 3$) are installed in a DN with three predefined loading levels (i. e., $N_{LV} = 3$), the total number of decision variables is 15. Furthermore, if the DN considers hourly loading variations (i. e., $N_{LV} = 24$), the number of decision variables increases to 78. This structure ensures that the proposed IAHA optimizes SVC placement, sizing, and reactive power compensation to maximize energy savings and voltage stability while maintaining cost effectiveness.

A. Equality Constraints

The SVC is essential in the shunt-linked device group of flexible AC transmission system (FACTS) devices. Grid voltage can be actively adjusted based on its level parameters through producing (capacitive) and absorbing (inductive) reactive power. Because of the short-term response and dynamic performance of SVC, operators can vary the angles and amplitudes of the internal voltage to manage the voltage values at the point of common coupling [38]. To implement the SVC model in a DN, the entire limit of load flow balance is updated at all loading levels, which can be given as:

$$P_{Grid,LV} = P_{Losses,LV} + \sum_{I=1}^{N_{svc}} Pd_{bus_I,LV} \quad LV \in [1, N_{LV}] \quad (3)$$

$$\sum_{I=1}^{N_{svc}} (Qsvc_{bus_I,LV}) + Q_{Grid,LV} = Q_{Losses,LV} + \sum_{I=1}^{N_{svc}} Qd_{bus_I,LV} \quad LV \in [1, N_{LV}] \quad (4)$$

where $P_{Grid,LV}$ and $Q_{Grid,LV}$ are the active and reactive power provided by the grid at loading level LV, respectively; $P_{losses,LV}$ is the total system active power loss at loading level LV; $Q_{losses,LV}$ is the total system reactive power loss at loading level LV; and $Pd_{bus_I,LV}$ is the real power demand at bus I at loading level LV.

B. Inequality Constraints

The decision variables in (2) should be maintained within permissible limits. The candidate bus to install SVC is an integer variable, except for the first substation-related bus (5). In addition, the SVC capacity potential must be less than the maximum rate (6).

$$2 \geq bus_I \geq N_{buses} \quad I \in [1, N_{svc}] \quad (5)$$

$$Qsvc^{\max,Rate} \geq Qsvc_{bus_I}^{Rate} \quad I \in [1, N_{svc}] \quad (6)$$

where N_{buses} is the number of buses in the DN; and $Qsvc^{\max,Rate}$ is the maximum rated SVC capacity.

For each hourly loading level, the ability of an SVC to change its outputs to absorb and inject reactive power simultaneously during the day and night is within a specified rated capacity $Qsvc_{bus_I}^{Rate}$, which can be expressed as:

$$-Qsvc_{bus_I}^{Rate} \leq Qsvc_{bus_I,LV} \leq Qsvc_{bus_I}^{Rate} \quad LV \in [1, N_{LV}], I \in [1, N_{svc}] \quad (7)$$

Additionally, the voltages of all terminals at each hourly loading level must always adhere to the permitted limits [39], which are given as:

$$V_q^{\max} \leq V_{q,LV} \leq V_q^{\min} \quad LV \in [1, N_{LV}], q = [1, N_{buses}] \quad (8)$$

where $V_q^{\max}$ and $V_q^{\min}$ are the maximum and minimum voltage margins for bus q, with their allowable range being 10%, respectively.

At each loading level LV, the current flow across the entire DN branch must always be less than the safe thermal limit, which can be given as:

$$-I_{Line}^{\max} \leq I_{Line,LV} \leq I_{Line}^{\max} \quad LV \in [1, N_{LV}], Line \in [1, N_{lines}] \quad (9)$$

where $I_{Line}^{\max}$ is the safe thermal limit of the DN branch; N_{lines} is the total number of DN branches; and $I_{Line,LV}$ is the current flow of the DN branch at loading level LV.

III. Solution Based on Proposed IAHA

In AHA, a swarm of hummingbirds is initially randomly assigned to B_n food sources, which is given as:

$$Bh_k = Lo + Rand(Up - Lo) \quad \forall k \in B_n \quad (10)$$

where Lo and Up are the lowest and highest limits of the decision variables, respectively; Bh_k is the location of the k^{th} food source, which represents a solution; and $Rand$ denotes a random variable in [0,1].

To imitate hummingbird memory of the period during which each food source remains unvisited, a feeding source visit table is expressed as:

$$VSTT_{k,j} = \begin{cases} \text{null} & k = j, j \in [1, B_n], k \in [1, B_n] \\ 0 & k \neq j, j \in [1, B_n], k \in [1, B_n] \end{cases} \quad (11)$$

where $VSTT_{k,j}$ is the time interval number throughout which a hummingbird j does not visit the k^{th} food source; and null

denotes lack of information.

Axial, omnidirectional, and diagonal movements are examples of flight abilities of AHA during foraging [26]. Hummingbirds employ a guided technique to investigate a specific food source, eventually discovering a potential source as:

$$Bhnew_k(it+1)=Bh_{k,target}(it)+(Bh_k(it)-Bh_{k,target}(it))\cdot FD\cdot a \tag{12}$$

where a is a flight parameter, which is a random value following a Gaussian distribution [0, 1]; $Bh_k(it)$ and $Bh_{k,target}(it)$ are the locations of the k^{th} food source correlated with the intended and available food sources at iteration it, respectively; FD is the flying direction; and $Bhnew_k(it+1)$ is the new location of the k^{th} food source at iteration $it+1$.

In the second step, hummingbirds use a territorial foraging pattern to look for progressively developed food sources within their territory, which is given as:

$$Bhnew_k(it+1)=Bh_k(it)(1+N(0,1)\cdot FD) \tag{13}$$

where $N(0,1)$ is the Gaussian distribution.

The mechanism for altering the location of each food source is expressed as:

$$Bh_k(it+1)=\begin{cases} Bhnew_k(it+1) & TF(Bhnew_k(it+1))<TF(Bh_k(it)) \\ Bh_k(it) & TF(Bhnew_k(it+1))\geq TF(Bh_k(it)) \end{cases} \tag{14}$$

where $TF(\cdot)$ denotes the target value of objective function (1).

Thus, the hummingbird decides to forsake the current food source and searches for a projected food source to eat if the nectar refilling rates of the acquired food source are greater than the existing rates.

Hummingbirds fly to a randomly selected fresh food source from the complete exploring universe if a food source is depleted in its surroundings [26], which is given as:

$$FD_k=\begin{cases} 1 & k=P(j),P=rndperm(x),j\in[1,m],x\in[2,1+r(dim-2)] \\ 0 & \text{else} \end{cases} \tag{15}$$

$$FD_k=\begin{cases} 1 & k=rnd_i(1,dim) \\ 0 & \text{else} \end{cases} \tag{16}$$

$$FD_k=1 \quad k\in[1,dim] \tag{17}$$

where FD_k is the k^{th} food source; m is a random integer; $rndperm(x)$ is the permutation function of random integer x; $rnd_i(\cdot)$ is the function used to generate random integer; dim is the number of dimensions; and r is an arbitrary number in [0, 1].

Each hummingbird must constantly explore within a specific search region. However, any decision variable that does not meet this criterion should be forwarded to the search region limit, which is given as:

$$Bh_k^{(i)}(it+1)=\begin{cases} Lo^{(i)} & Bh_j^{(i)}(it+1)<Lo^{(i)} \\ Up^{(i)} & Bh_j^{(i)}(it+1)>Up^{(i)} \quad k\in[1,B_n],i\in dim \\ Bh_k^{(i)}(it+1) & \text{else} \end{cases} \tag{18}$$

where superscript (i) denotes the dimension of each design variable.

The feeding source visit table is an important aspect of conventional AHA for tracking the trajectories toward food sources. Each hummingbird can select its favored food source by evaluating it frequently [27]. Thus, (11) can be adjusted as:

$$VSTT_{k,j}=VSTT_{k,j}+1 \quad j\neq k,j\neq target,j\in[1,B_n] \tag{19}$$

$$VSTT_{k,target}=0 \tag{20}$$

$$VSTT_{k,j}=\max_{L\neq k,L\in[1,B_n]}(VSTT_{k,L})+1 \quad j\neq k,j=[1,B_n] \tag{21}$$

where *target* is the favored food source.

The proposed IAHA includes several modifications to enhance the performance of the conventional AHA. The directed foraging pattern considerably improves, which is given as:

$$Bhnew_k(it+1)=(Bh_k(it)-Bh_m(it))a\cdot FD+Bh_{k,target}(it) \tag{22}$$

$$m=rand_i(1,B_n) \quad m\neq k \tag{23}$$

where $rand_i(\cdot)$ denotes a uniform distribution function to generate a pseudorandom integer within the food souce B_n.

Directed foraging pattern is promoted by guiding the search pathways out of the optimal solution and into various alternative directions near other hummingbirds at each iteration. Only the most relevant locations for hummingbird foraging are identified. Hence, the exploitative behavior can be justified. Territory foraging patterns are incorporated into the territorial foraging pattern as:

$$Bhnew_k(it+1)=\begin{cases} Bh_k(it)+b\cdot FD\cdot Bh_k(it) & rand<\dfrac{1}{3} \\ Bh_k(it)+b\cdot FD\cdot(Bh_k(it)-Bh_m(it)) & \dfrac{1}{3}\leq rand<\dfrac{2}{3} \\ Bh_m(it)+b\cdot FD\cdot(Bh_k(it)-Bh_m(it)) & rand\geq\dfrac{2}{3} \end{cases} \tag{24}$$

where *rand* is a randomized value within range [0, 1]; and b is a territorial parameter that takes a random value following a Gaussian distribution function.

The territorial foraging pattern is enhanced in the proposed IAHA by transferring different and fluctuating knowledge from surrounding hummingbirds instead of depending solely on individual hummingbird experiences. As a result, hummingbirds are better equipped to look for a food source in their vicinity.

Equation (25) describes a linear regulation with adjustable parameter ψ, which increases linearly with iterations. Thus, ψ limits the exploitative behavior and hummingbird foraging activity. Territory foraging pattern described by (24) is employed by all hummingbirds in the beginning and demonstrates 100% exploratory behavior. Exploitation using directed foraging pattern described by (22) increases, whereas exploration in territory foraging pattern described by (24) decreases with increasing the magnitude of parameter ψ.

$$\psi=\frac{it}{\max it} \tag{25}$$

The proposed IAHA addresses the time-dependent operational allocation of SVCs in DNs, as depicted in Fig. 1.

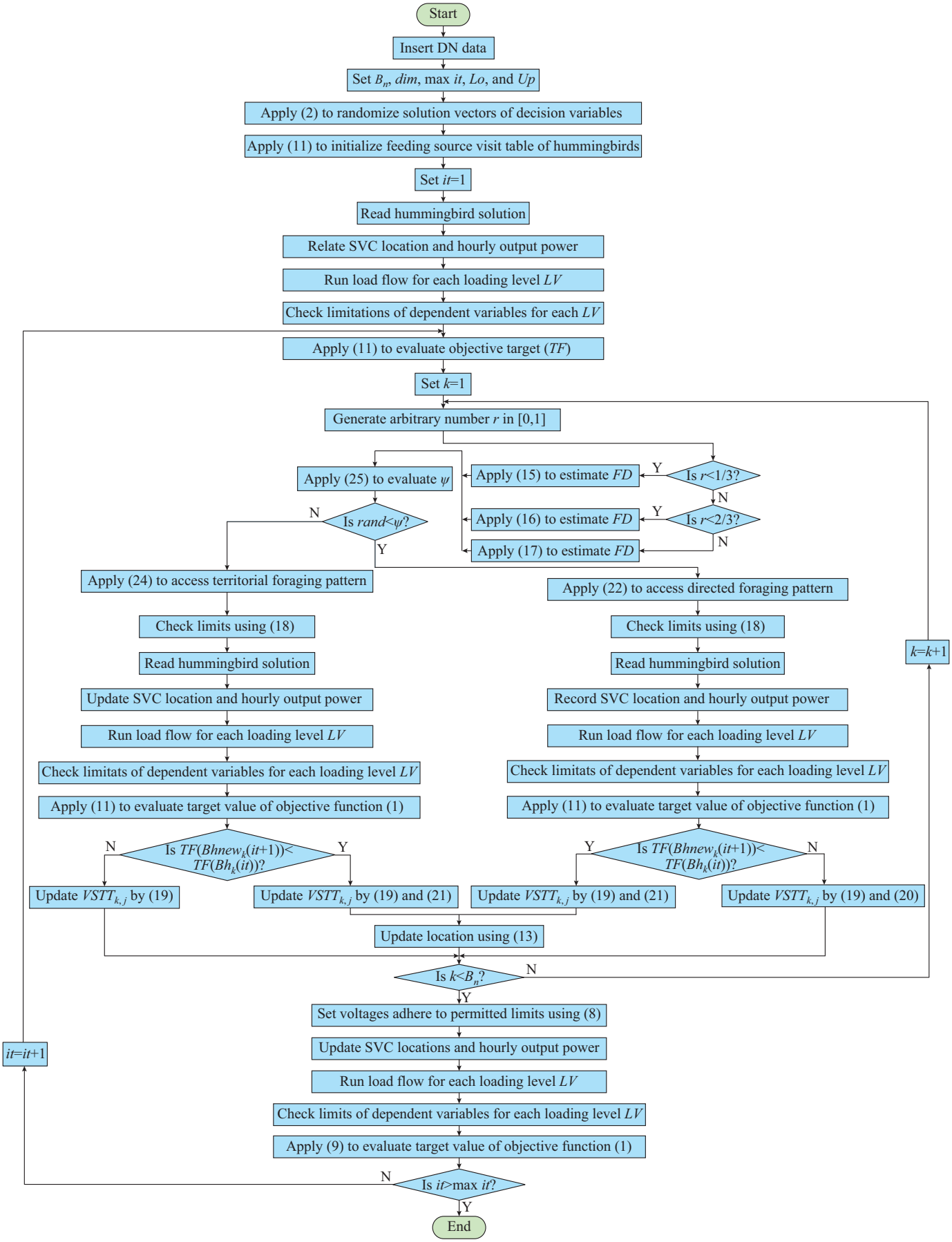

Fig. 1. Flowchart of proposed IAHA for solving time-dependent operational allocation of SVCs in DNs.

IV. Simulation Results

The proposed IAHA is evaluated on IEEE DN models with 33 and 69 nodes (IEEE 33-bus DN and IEEE 69-bus DN, respectively). Three different loading levels are used, with each receiving a daily supply of 8 hours. Low, medium, and high loading conditions (loading levels) are managed at 60%, 80%, and 100% of nominal loading, respectively [40]. The maximum number of SVCs for placement is three. The highest capacity of the inserted SVC is 3000 kvar. First, a compensation limit of 50% of the total reactive power consumption is considered across three loading levels. Second, the effects of varying the compensation limits on the performance of the system are analyzed. The proposed IAHA offers adaptive parameters for flight and territory while setting only iterations and solution individuals, which is similar to population metaheuristic algorithms. These two parameters are set and fixed for all evaluated algorithms. For both the proposed IAHA and conventional AHA, 20 search agents and 100 iterations are set while considering three loading levels, resulting in 15 decision variables. When the analysis is extended to account for 24-hour load variations, the number of decision variables increases to 78. The algorithms are implemented on a computer equipped with an Intel® Core™ i7-470K CPU at 4.00 GHz with 16.00 GB RAM.

A. IEEE 33-bus DN

The first evaluated DN has 33 nodes, 32 sections, and a typical operating voltage of 12.66 kV. Regarding the nominal conditions, the total active, reactive, and apparent loads are 3.715 MW, 2.3 Mvar, and 4.369 MVA, respectively [41].

1) Loading Levels in IEEE 33-bus DN

In this part, 50% of the total reactive power consumption is considered as the maximum financial limit. The proposed IAHA is used and compared with the conventional AHA, GBO, HBA, DMOA, SSA, and DE algorithm. Table I lists the allocations of SVCs (IEEE 33-bus DN). Figrue 2 shows the convergence characteristics of various algorithms (IEEE 33-bus DN). As indicated in Table I and Fig. 2, the proposed IAHA achieves the highest annual cost saving of $21735.725 while demonstrating the highest performance. The conventional AHA provides annual cost saving of $21672.883, ranking second. While the GBO ranks third with annual cost saving of $21474.100. In addition, the DE algorithm, HBA, and DMOA rank fourth, fifth, and sixth with annual cost saving of $21466.900, $21078.800, and $21015.600, respectively. SSA has the lowest efficiency of the evaluated algorithms, with annual cost saving of $15131.600.

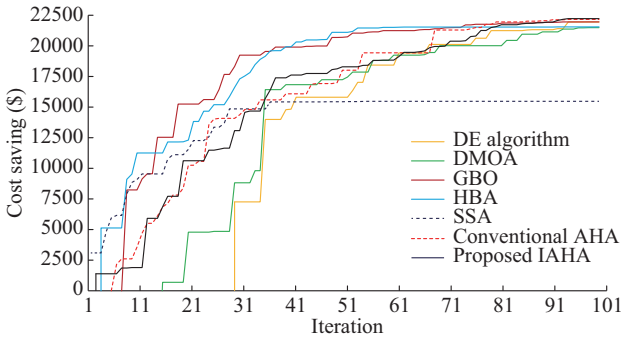

Fig. 2. Converging features of various algorithms (IEEE 33-bus DN).

TABLE I
Allocations of SVCs (IEEE 33-bus DN)

Algorithm	Annual cost saving ($)	Allocation of SVCs		Operational value (kvar)		
		Number of installed buses	Rated value (kvar)	High	Medium	Low
AHA	21672.883	10	±130	130	127	102
		17	±181	46	171	181
		30	±804	717	824	804
Proposed IAHA	21735.725	11	±321	232	292	321
		17	±135	94	117	135
		30	±692	615	692	676
GBO	21474.100	7	±116	113	116	–33
		16	±136	136	134	124
		30	±898	898	855	739
DMOA	21015.600	9	±328	328	285	165
		14	±147	145	147	121
		30	±651	583	651	511
SSA	15131.600	30	±574	574	247	181
		32	±239	199	194	239
HBA	21078.800	13	±289	289	269	–29
		30	±831	831	771	811
DE algorithm	21466.900	16	±279	264	206	279
		30	±588	588	471	467
		31	±271	271	271	228

Figure 3 shows the voltage profile using the proposed IAHA versus conventional AHA (IEEE 33-bus DN), where initial scenario denotes the initial topology of the system without adding any devices. The proposed IAHA demonstrates significant voltage improvement across all loading buses for three loading levels compared with conventional AHA. Specifically, the proposed IAHA increases the minimum voltages by 2.59%, 2.34%, and 1.89%, elevating the voltage magnitudes from 0.9037, 0.9244, and 0.944 (conventional AHA) to 0.927, 0.946, and 0.962 at high, medium, and low loading levels, respectively.

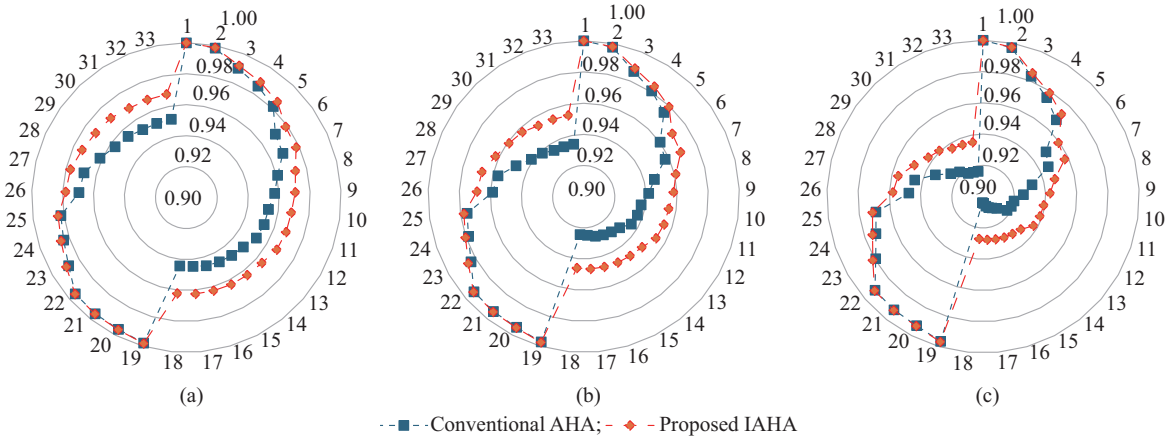

Fig. 3. Voltage profile based on proposed IAHA versus conventional AHA (IEEE 33-bus DN). (a) Low level. (b) Medium level. (c) High level.

Figure 4 shows a boxplot of cost savings of various algorithms. Table II shows the robustness metrics of cost savings of various algorithms (IEEE 33-bus DN). The proposed IAHA demonstrates superior performance and robustness compared with other algorithms, achieving the highest annual cost saving. The proposed IAHA achieves the best, average, and worst annual cost savings of $21735.7, $20921.1, and $19257.1, respectively. According to the average annual cost saving, DE algorithm ranks second with annual cost savings of $20318.0, whereas the conventional AHA ranks third with annual cost savings of $20051.4.

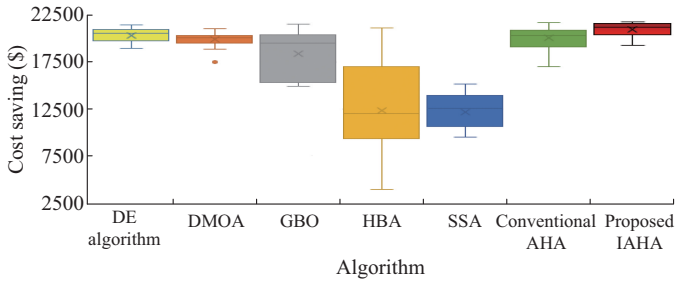

Fig. 4. Boxplot of cost savings of various algorithms (IEEE 33-bus DN).

Compared with the conventional AHA, the proposed IAHA shows a small improvement of 0.29% in the best annual cost saving. Nevertheless, the proposed IAHA provides large improvements of 4.16%, 11.67%, and 37.91% for the average annual cost saving, worst annual cost saving, and standard deviation, respectively. On one hand, the computational time required for each algorithm highlights the efficiency of the proposed IAHA in solving the optimization problem of the IEEE 33-bus DN. The proposed IAHA has a computational time of 11.63 s, being comparable with that of other algorithms such as DE algorithm (11.82 s), AHA (11.66 s), and SSA (10.99 s). On the other hand, a longer computational time of 20.21 s is required by DMOA. This increase is due to the double-function evaluation per solution, whereas the other algorithms require a single function evaluation per iteration.

TABLE II
ROBUSTNESS METRICS OF VARIOUS ALGORITHMS (IEEE 33-BUS DN)

Algorithm	Annual cost saving ($)			Standard deviation ($)	Computational time (s)
	Best	Average	Worst		
DE algorithm	21466.9	20318.0	18907.0	781.89	11.82
DMOA	21015.6	19897.4	17508.6	862.88	19.52
GBO	21474.1	18339.0	14902.5	2528.66	12.53
HBA	21078.8	12322.9	3967.0	4818.64	11.94
SSA	15131.6	12202.0	9546.8	1695.28	10.99
Conventional AHA	21672.9	20051.5	17009.1	1268.23	11.66
Proposed IAHA	21735.7	20921.1	19257.1	787.44	11.63

To evaluate the impacts of variations in the compensation limits on system performance, we analyse the proposed IAHA across compensation limits ranging from 50% to 100% of the total reactive power load in 10% increments. The proposed IAHA is applied to each compensation limit, and the annual cost savings are shown in Fig. 5.

Increasing in the maximum reactive power compensation limit enhances annual cost savings, but the improvement rates vary significantly. For compensation limit increases from 50% to 60% of the total reactive power load, the annual cost saving increases from $21735.72 to $22935.8, that is, an improvement rate of 5.23%. For compensation limit increases from 60% to 70% of the total reactive power load, the annual cost saving increases by 2.74%, whereas the annual cost saving increases by 2.3% when the compensation limit increases from 70% to 80% of the total reactive power

load. In contrast, the improvement rate substantially decreases to 0.97% and 0.49%, respectively, when the compensation limit increases from 90% to 100% of the total reactive power load.

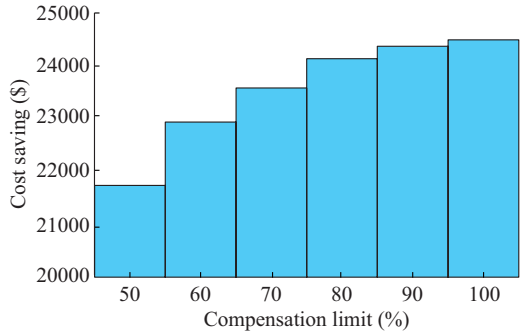

Fig. 5. Annual cost saving of proposed IAHA under different compensation limits (IEEE 33-bus DN).

Figures 6 and 7 show the power losses and the minimum voltage related to each loading level of different compensation limits (IEEE 33-bus DN). Large improvements in power losses and the minimum voltages are observed at all loading levels.

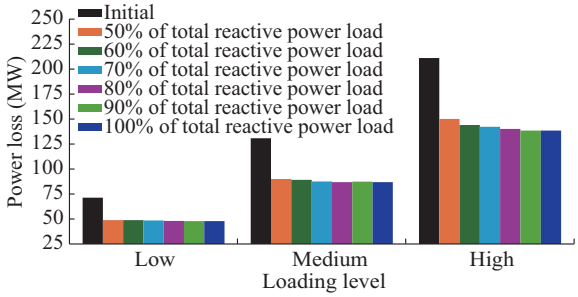

Fig. 6. Power losses related to each loading level of different compensation limits (IEEE 33-bus DN).

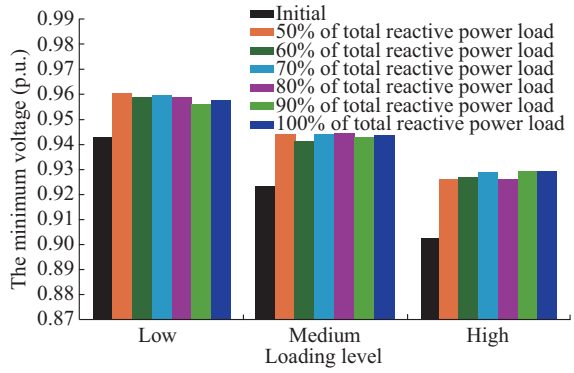

Fig. 7. The minimum voltage related to each loading level of different compensation limits (IEEE 33-bus DN).

2) Hourly Loading Variation in IEEE 33-bus DN

The proposed IAHA is used to perform time-dependent operational allocation of SVCs considering hourly loading variation. The amount of compensation limit is fixed at 80% of the total reactive power load. Figure 8 shows hourly loading profile in terms of the percentage of nominal loading condition. A comparative analysis between the proposed IAHA and the conventional AHA is conducted, with the corresponding convergence characteristics in terms of annual cost savings depicted in Fig. 9. The results demonstrate that the proposed IAHA achieves faster convergence, yielding an annual cost saving of $22965.74, whereas the conventional AHA achieves $22534.09, representing a 1.91% improvement in annual cost saving.

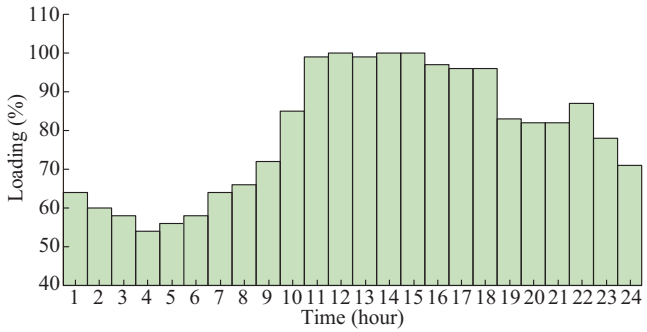

Fig. 8. Hourly loading profile in terms of percentage of nominal loading condition.

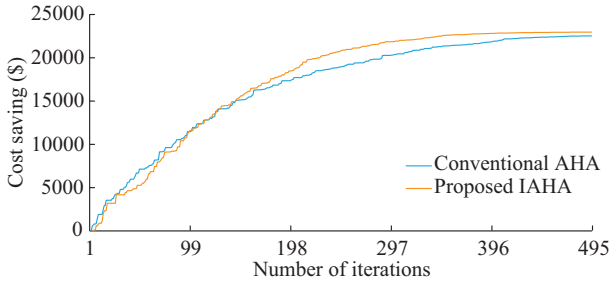

Fig. 9. Convergence characteristics of conventional AHA and proposed IAHA (IEEE 33-bus DN).

The outputs are adjusted throughout the day by injection of reactive power. The SVCs operate in the reactive power injection mode throughout the day. Their reactive power outputs remain at high levels of more than 95% of their specified capacities during the operating hours (11: 00-18: 00), which corresponds to the high loading level. Figure 10 shows the reactive power compensation of the proposed IAHA under hourly loading variation.

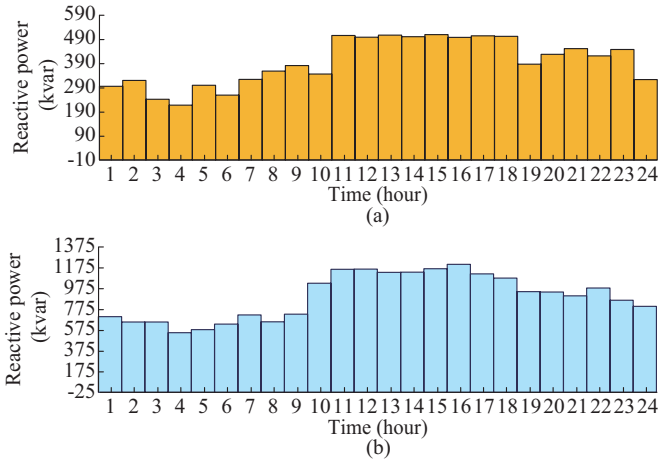

Fig. 10. Reactive power compensation of proposed IAHA under hourly loading variation (IEEE 33-bus DN). (a) Bus 12. (b) Bus 30.

In addition, Fig. 11 shows the improvements in power loss and the minimum voltage of the proposed IAHA. The proposed IAHA achieves consistent hourly power loss reductions exceeding 31%. Similarly, a large increase in the minimum voltage is achieved, ranging from 1.24% to 2.89% at 04:00 and 16:00, respectively.

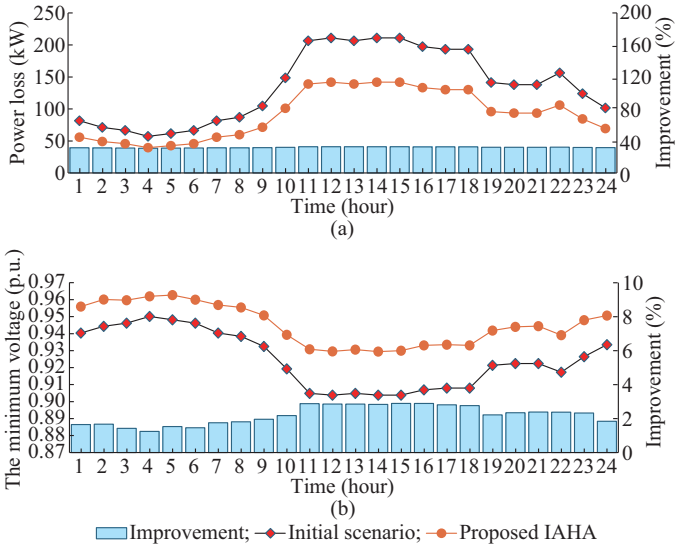

Fig. 11. Improvements in power losses and the minimum voltage of proposed IAHA (IEEE 33-bus DN). (a) Power loss. (b) The minimum voltage.

B. IEEE 69-bus DN

In this subsection, the evaluated DN has 69 distribution nodes and 68 sections, with a typical operating voltage of 12.66 kV. For the nominal condition, the total active and reactive loads are 3.8021 MW and 2.6947 Mvar, respectively [42].

1) Loading Levels in IEEE 69-bus DN

As for the IEEE 33-bus DN, 50% of the total reactive power load is considered as the maximum financial limit. Table III lists the allocations of SVCs and annual cost savings. Figure 12 shows convergence characteristics of different algorithms (IEEE 69-bus DN). The proposed IAHA achieves the highest annual cost saving of $24262.04 while demonstrating the highest performance. The conventional AHA ranks second with annual cost saving of $23791.3, while the GBO ranks third with annual cost saving of $23567.079. In addition, DE algorithm, DMOA, and HBA rank fourth, fifth, and sixth with annual cost savings of $22789.45, $22451.285, and $21036.073, respectively. It is worth noting that, SSA provides the lowest efficiency of various algorithms, with the annual cost saving of $18007.217.

Figure 13 shows a boxplot of cost savings of various algorithms (IEEE 69-bus DN). Table IV highlights the robustness metrics of various algorithms. Despite the moderate computational time (13.36 s), the proposed IAHA outperforms the other algorithms in terms of robustness metrics, achieving the highest best, average, and worst annual cost savings ($24262.04, $23190.72, and $21796.22, respectively) while maintaining the lowest standard deviation ($742.112). While the proposed IAHA demonstrates a modest 1.94% improvement in the best annual cost savings compared with the conventional AHA, it substantially outperforms conventional AHA regarding the average annual cost saving, worst annual cost saving, and standard deviation by 5.67%, 23.9%, and 61.79%, respectively. This suggests that the proposed IAHA provides superior optimization performance without excessive computational overhead, making it practical and efficient for real-world power system applications.

TABLE III
ALLOCATIONS OF SVCS AND ANNUAL COST SAVINGS (IEEE 69-BUS DN)

Algorithm	Annual cost saving ($)	Allocation of SVCs		Operational value (kvar)		
		Installed node	Rated value (kvar)	High	Medium	Low
Conventional AHA	23791.30	14	±183	146	183	102
		61	±827	827	788	766
		64	±126	126	94	125
Proposed IAHA	24262.04	19	±223	223	181	207
		61	±685	685	677	579
		64	±241	237	241	194
DE algorithm	22789.45	62	±557	557	452	332
		63	±484	382	484	383
		69	±82	82	82	59
DMOA	22451.28	62	±393	393	358	275
		63	±416	236	416	261
		64	±332	309	332	303
SSA	18007.22	61	±701	324	467	701
		64	±259	259	154	211
HBA	21036.07	61	±321	321	321	96
		62	±618	618	618	277
GBO	23567.08	21	±189	189	165	149
		61	±876	876	876	781

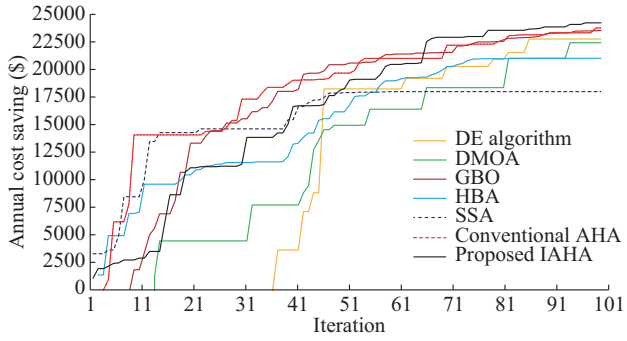

Fig. 12. Convergence characteristics of various algorithms (IEEE 69-bus DN).

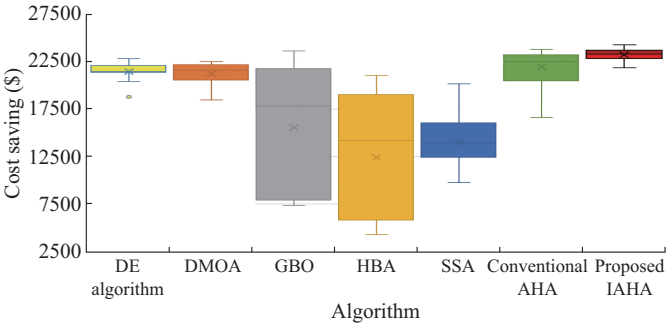

Fig. 13. Boxplot of cost savings of various algorithms (IEEE 69-bus DN).

TABLE IV
ROBUSTNESS METRICS OF VARIOUS ALGORITHMS (IEEE 69-BUS DN)

Algorithm	Annual cost saving ($)			Standard deviation ($)	Computational time (s)
	Best	Average	Worst		
DE algorithm	22789.5	21455.4	18809.30	941.67	12.97
DMOA	22451.3	21174.1	18440.70	1290.25	20.21
GBO	23567.1	15569.1	7395.12	6708.39	13.82
HBA	21036.1	12437.8	4269.26	6815.09	13.01
SSA	20167.7	14045.6	9787.98	2705.18	12.06
Conventional AHA	23791.3	21875.4	16587.70	1942.02	13.24
Proposed IAHA	24262.0	23190.7	21796.20	742.11	13.36

The proposed IAHA is used to analyze the impact of varying compensation limits on the system performance. We analyse the proposed IAHA across compensation limits ranging from 50% to 100% of the total reactive power load in 10% increments. Figure 14 shows the annual cost saving of proposed IAHA under different compensation limits (IEEE 69-bus DN).

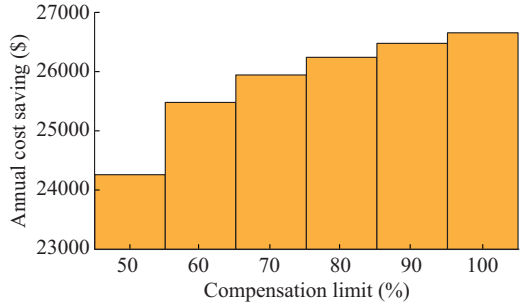

Fig. 14. Annual cost saving of proposed IAHA under different compensation limits (IEEE 69-bus DN).

Higher compensation limits generally result in the increase in annual cost savings, but the improvement rate decreases as the compensation limit increases. Annual cost savings grow considerably by 4.79% when the compensation limit increases from 50% to 60% of the total reactive power load and by 1.79% from 60% to 70% of the total reactive power load. However, the improvement is reduced to 1.13%, 0.89%, and 0.67% for the subsequent 10% increments up to 100%.

2) Hourly Loading Variation in IEEE 69-bus DN

In this part, the proposed IAHA and conventional AHA are used for evaluation. Figure 15 shows the convergence characteristics of the proposed IAHA and conventional AHA.

The proposed IAHA reduces the annual cost by $26050.05, while the conventional AHA provides annual cost saving of $24957.44, that is, a 4.37% increase in cost. Figure 16 shows the benefits of power loss and the minimum voltage provided by the proposed IAHA per hourly load. A substantial decrease in power loss is obtained per hour, which reaches at least 33.2%. Similarly, the lowest voltage increases considerably with each hour, ranging from 1.14% to 2.31% at 04:00 and 11:00, respectively.

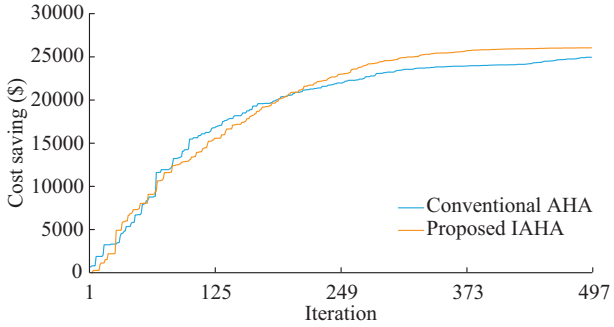

Fig. 15. Convergence characteristics of conventional AHA and proposed IAHA (IEEE 69-bus DN).

Figure 16 shows the reactive power compensation of the proposed IAHA under hourly loading variation (IEEE 69-bus DN), which requires the installation of three SVCs at buses 18, 61, and 62 and specifies the operating outputs of the SVCs per hour. Their outputs adapt during the day under a heavy supply of reactive power. Figure 17 shows the improvements in power losses and the minimum voltage of proposed IAHA (IEEE 69-bus DN).

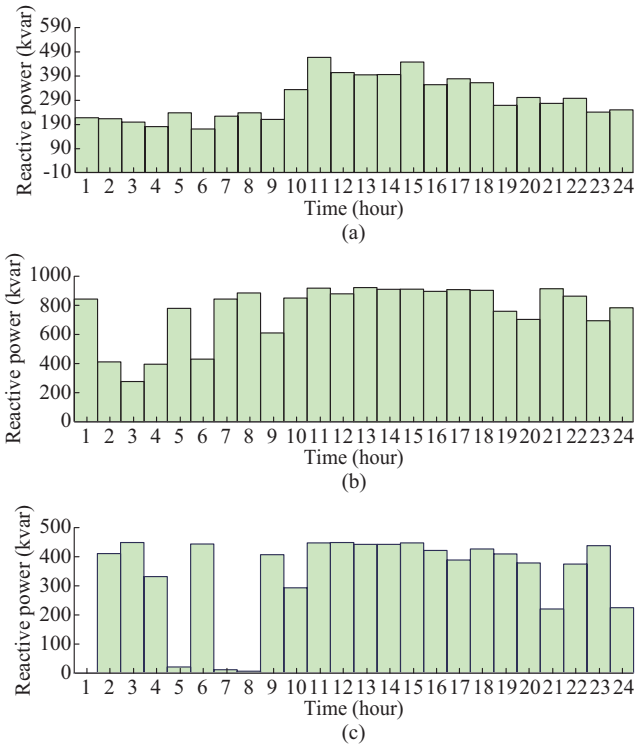

Fig. 16. Reactive power compensation of proposed IAHA under hourly loading variation (IEEE 69-bus DN). (a) Bus 18. (b) Bus 61. (c) Bus 62.

V. CONCLUSION

This paper presents an IAHA for the optimal placement and sizing of SVCs aimed at maximizing the annual cost savings in power loss and improving the voltage profile. The proposed IAHA simultaneously considers several loading levels. In addition, the SVC outputs are modulated by the loading level. Furthermore, the installed SVC ratings are treated as supplementary constraints related to the compensation levels of the overall reactive demand to reflect the financial in-

stallation capacity. The applicability of the proposed IAHA is evaluated using the IEEE 33- and 69-bus DNs. The simulation results show that the proposed IAHA outperforms the conventional AHA and other state-of-the-art algorithms in terms of annual cost savings. Moreover, a large increase in the hourly minimum voltage is achieved. Varying compensation levels reveals that increasing the maximum reactive power compensation limit leads to higher cost savings. However, the benefits decrease as the compensation level increases, emphasizing the need for balanced compensation.

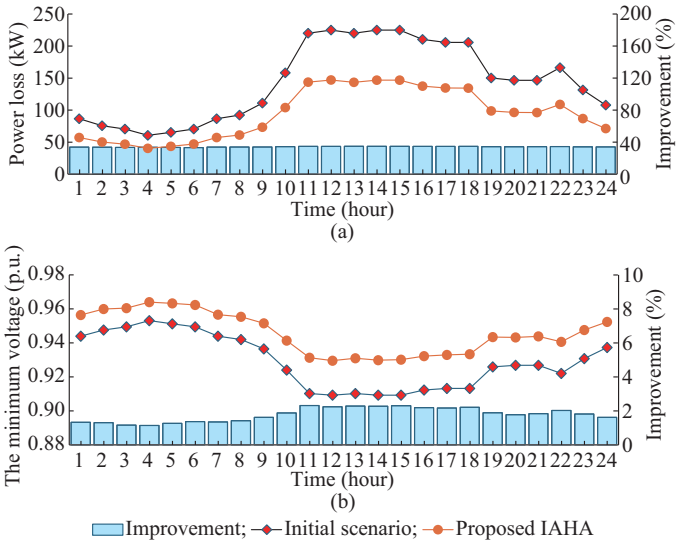

Fig. 17. Improvements in power losses and the minimum voltage of proposed IAHA (IEEE 69-bus DN). (a) Power loss. (b) The minimum voltage.

Although the proposed IAHA enhances SVC allocation, savings, and voltage regulation, it has some limitations. Equipment aging, maintenance, failure, harmonic distortion, transient stability, and power quality issues remain to be addressed. In addition, the validation is limited to the IEEE 33-bus and 69-bus DNs, leaving its scalability to larger networks untested. Additionally, we did not evaluate the impact of renewable energy sources on reactive power compensation. Although hourly load variations are considered, real-world demand patterns influenced by weather and consumer behavior remain to be studied. Future research can further refine the proposed IAHA by addressing its limitations and expanding its applicability. It can incorporate equipment aging, maintenance schedules, and failure models to improve the long-term reliability of SVC allocation. Analyzing the impact of SVC operation on power quality issues will enable a more comprehensive performance assessment. Validating the scalability of the proposed IAHA in large-scale DNs and integrating renewable energy sources will lead to more adaptive compensation strategies. Furthermore, exploring machine learning for load forecasting and stochastic optimization will likely enhance the effectiveness of the proposed IAHA.

REFERENCES

[1] A. Eid, S. Kamel, A. Korashy *et al.*, "An enhanced artificial ecosystem-based optimization for optimal allocation of multiple distributed generations," *IEEE Access*, vol. 8, pp. 178493-178513, Sept. 2020.

[2] P. Li, H. Dong, G. Zhang *et al.*, "Research on loss reduction strategy of distribution network based on distributed generation site selection and capacity," *Energy Reports*, vol. 9, pp. 1001-1012, Sept. 2023.

[3] Y. Wang, Y. Xu, J. Li *et al.*, "On the radiality constraints for distribution system restoration and reconfiguration problems," *IEEE Transactions on Power Systems*, vol. 35, no. 4, pp. 3294-3296, Jul. 2020.

[4] D. Ćetković and V. Komen, "Optimal distributed generation and capacitor bank allocation and sizing at two voltage levels," *IEEE Systems Journal*, vol. 17, no. 4, pp. 5831-5841, Dec. 2023.

[5] S. Hu, Y. Xiang, X. Zhang *et al.*, "Reactive power operability of distributed energy resources for voltage stability of distribution networks," *Journal of Modern Power Systems and Clean Energy*, vol. 7, no. 4, pp. 851-861, Jul. 2019.

[6] Prashant, A. Siddiqui, and M. Sarwar, "Locational marginal pricing based management of congestion with optimum sizing of distributed generator using modified ILSHADE algorithm," in *Proceedings of 2022 International Conference on Electronic Systems and Intelligent Computing*, Chennai, India, Apr. 2022, pp. 317-322.

[7] A. Shaheen, A. Elsayed, A. Ginidi *et al.*, "Effective automation of distribution systems with joint integration of DGs/SVCs considering reconfiguration capability by jellyfish search algorithm," *IEEE Access*, vol. 9, pp. 92053-92069, Jun. 2021.

[8] E. Elattar, A. Shaheen, A. El-Sayed *et al.*, "Optimal operation of automated distribution networks based-MRFO algorithm," *IEEE Access*, vol. 9, pp. 19586-19601, Jan. 2021.

[9] M. Behbahani, A. Jalilian, A. Bahmanyar *et al.*, "Comprehensive review on static and dynamic distribution network reconfiguration methodologies," *IEEE Access*, vol. 12, pp. 9510-9525, Jan. 2024.

[10] H. Arasteh, M. Sepasian, and V. Vahidinasab, "An aggregated model for coordinated planning and reconfiguration of electric distribution networks," *Energy*, vol. 94, pp. 786-798, Jan. 2016.

[11] A. Abdelsalam and H. Mansour, "Optimal allocation and hourly scheduling of capacitor banks using sine cosine algorithm for maximizing technical and economic benefits," *Electric Power Components and Systems*, vol. 47, no. 11-12, pp. 1025-1039, Jul. 2019.

[12] N. Khan, Y. Wang, D. Tian *et al.*, "A novel modified lightning attachment procedure optimization technique for optimal allocation of the FACTS devices in power systems," *IEEE Access*, vol. 9, pp. 47976-47997, Feb. 2021.

[13] M. Kamarposhti, H. Shokouhandeh, I. Colak *et al.*, "Optimal location of FACTS devices in order to simultaneously improving transmission losses and stability margin using artificial bee colony algorithm," *IEEE Access*, vol. 9, pp. 125920-125929, Aug. 2021.

[14] I. Soesanti and R. Syahputra, "Multiobjective ant lion optimization for performance improvement of modern distribution network," *IEEE Access*, vol. 10, pp. 12753-12773, Jan. 2022.

[15] M. Alvarez-Alvarado, C. Rodríguez-Gallegos, and D. Jayaweera, "Optimal planning and operation of static VAR compensators in a distribution system with non-linear loads," *IET Generation, Transmission & Distribution*, vol. 12, no. 15, pp. 3726-3735, Aug. 2018.

[16] A. Savić and Ž. Đurišić, "Optimal sizing and location of SVC devices for improvement of voltage profile in distribution network with dispersed photovoltaic and wind power plants," *Applied Energy*, vol. 134, pp. 114-124, Dec. 2014.

[17] D. Thukaram and A. Lomi, "Selection of static VAR compensator location and size for system voltage stability improvement," *Electric Power Systems Research*, vol. 54, no. 2, pp. 139-150, May 2000.

[18] B. Singh and G. Agrawal, "Enhancement of voltage profile by incorporation of SVC in power system networks by using optimal load flow method in MATLAB/Simulink environments," *Energy Reports*, vol. 4, pp. 418-434, Nov. 2018.

[19] A. Eid, S. Kamel, H. Zawbaa *et al.*, "Improvement of active distribution systems with high penetration capacities of shunt reactive compensators and distributed generators using bald eagle search," *Ain Shams Engineering Journal*, vol. 13, no. 6, p. 101792, Nov. 2022.

[20] H. Merah, A. Gacem, D. Ben Attous *et al.*, "Sizing and sitting of static VAR compensator (SVC) using hybrid optimization of combined cuckoo search (CS) and antlion optimization (ALO) algorithms," *Energies*, vol. 15, no. 13, p. 4852, Jul. 2022.

[21] M. Zaidan and S. Toos, "Optimal location of static var compensator to regulate voltage in power system," *IETE Journal of Research*, vol. 69, no. 4, pp. 2177-2185, May 2023.

[22] R. Huang, W. Gao, R. Fan *et al.*, "A guided evolutionary strategy based-static var compensator control approach for interarea oscillation damping," *IEEE Transactions on Industrial Informatics*, vol. 19, no. 3, pp. 2596-2607, Mar. 2023.

[23] M. Djalal, I. Robandi, and M. Prakasa, "Stability enhancement of sulselrabar electricity system using mayfly algorithm based on static VAR compensator and multi-band power system stabilizer PSS2B," *IEEE Access*, vol. 11, pp. 57319-57340, May 2023.
[24] G. Moustafa, M. Elshahed, A. Ginidi *et al*., "A gradient-based optimizer with a crossover operator for distribution static VAR compensator (D-SVC) sizing and placement in electrical systems," *Mathematics*, vol. 11, no. 5, p. 1077, Mar. 2023.
[25] M. Taher, S. Kamel, F. Jurado *et al*., "Optimal locations and sizes of shunt FACT devices for enhancing power system loadability using improved moth flame optimization," *Electric Power Components and Systems*, vol. 49, no. 20, pp. 1536-1554, Dec. 2021.
[26] W. Zhao, L. Wang, and S. Mirjalili, "Artificial hummingbird algorithm: a new bio-inspired optimizer with its engineering applications," *Computer Methods in Applied Mechanics and Engineering*, vol. 388, p. 114194, Jan. 2022.
[27] A. Shaheen, A. Alassaf, I. Alsaleh *et al*., "Advancements in model parameter estimation for proton exchange membrane fuel cells via enhanced artificial hummingbird algorithm," *International Journal of Energy Research*, vol. 2024, no. 1, p. 7616065, Jan. 2024.
[28] A. Shaheen, A. Ginidi, A. Alassaf *et al*., "Developing artificial hummingbird algorithm with linear controlling strategy and diversified territorial foraging tactics for combined heat and power dispatch," *Alexandria Engineering Journal*, vol. 105, pp. 245-260, Oct. 2024.
[29] L. Li, B. Ji, Z. Li *et al*., "Microgrid energy management system with degradation cost and carbon trading mechanism: a multi-objective artificial hummingbird algorithm," *Applied Energy*, vol. 378, p. 124853, Jan. 2025.
[30] M. Hosseinzadeh, A. Rahmani, F. Husari *et al*., "A survey of artificial hummingbird algorithm and its variants: statistical analysis, performance evaluation, and structural reviewing," *Archives of Computational Methods in Engineering*, vol. 32, no. 1, pp. 269-310, Jan. 2025.
[31] B. Sasmal, A. Das, K. Dhal *et al*., "Artificial hummingbird algorithm: Theory, variants, analysis, applications, and performance evaluation," *Computer Science Review*, vol. 56, p. 100727, May 2025.
[32] R. Storn and K. Price, "Differential evolution – a simple and efficient heuristic for global optimization over continuous spaces," *Journal of Global Optimization*, vol. 11, no. 4, pp. 341-359, Dec. 1997.
[33] J. O. Agushaka, A. E. Ezugwu, and L. Abualigah, "Dwarf mongoose optimization algorithm," *Computer Methods in Applied Mechanics and Engineering*, vol. 391, p. 114570, Mar. 2022.
[34] S. Mirjalili, A. Gandomi, S. Mirjalili *et al*., "Salp swarm algorithm: a bio-inspired optimizer for engineering design problems," *Advances in Engineering Software*, vol. 114, pp. 163-191, Dec. 2017.
[35] L. Abualigah, M. Shehab, M. Alshinwan *et al*., "Salp swarm algorithm: a comprehensive survey," *Neural Computing and Applications*, vol. 32, no. 15, pp. 11195-11215, Nov. 2020.
[36] I. Ahmadianfar, O. Bozorg-Haddad, and X. Chu, "Gradient-based optimizer: a new metaheuristic optimization algorithm," *Information Sciences*, vol. 540, pp. 131-159, Nov. 2020.
[37] F. Hashim, E. Houssein, K. Hussain *et al*., "Honey badger algorithm: new metaheuristic algorithm for solving optimization problems," *Mathematics and Computers in Simulation*, vol. 192, pp. 84-110, Feb. 2022.
[38] S. Gasperic and R. Mihalic, "Estimation of the efficiency of FACTS devices for voltage-stability enhancement with PV area criteria," *Renewable and Sustainable Energy Reviews*, vol. 105, pp. 144-156, May 2019.
[39] A. M. El-Rifaie, A. M. Shaheen, M. A. Tolba *et al*., "Modified gradient-based algorithm for distributed generation and capacitors integration in radial distribution networks," *IEEE Access*, vol. 11, pp. 120899-120917, Oct. 2023.
[40] A. M. Shaheen, R. A. El-Sehiemy, S. Kamel *et al*., "Improving distribution networks' consistency by optimal distribution system reconfiguration and distributed generations," *IEEE Access*, vol. 9, pp. 67186-67200, Apr. 2021.
[41] A. M. Shaheen, A. M. Elsayed, A. R. Ginidi *et al*., "Improved heap-based optimizer for DG allocation in reconfigured radial feeder distribution systems," *IEEE Systems Journal*, vol. 16, no. 4, pp. 6371-6380, Dec. 2022.
[42] H. A. Khattab, A. S. Aljumah, A. M. Shaheen *et al*., "Improved manta ray foraging algorithm for optimal allocation strategies to power delivery capabilities in active distribution networks," *IEEE Access*, vol. 12, pp. 157699-157715, Oct. 2024.

Ali S. Aljumah received the B.Sc. degree in electrical engineering from the King Fahd University of Petroleum and Minerals (KFUPM), Dhahran, Saudi Arabia, in 2012, and the M.Sc. and Ph.D. degrees in electrical engineering from the University of South Florida (USF), Tampa, USA, in 2016 and 2022, respectively. Currently, he is an Assistant Professor with Department of Electrical Engineering, Prince Sattam Bin Abdulaziz University, Al Kharj, Saudi Arabia. His research interests include power system modeling, stability, and renewable energy source integration to power grid.

Mohammed H. Alqahtani received the B.S. degree in electrical engineering from Prince Sattam Bin Abdulaziz University, Al Kharj, Saudi Arabia, in 2012, the M.S. degree from the University of South Florida (USF), Tampa, USA, in 2016, and the Ph.D. degree from the Smart Grid Power Systems Laboratory, Tampa, USA, in 2021. He is currently an Assistant Professor with Prince Sattam Bin Abdulaziz University. His research interest includes power system computing and modeling.

Ahmed R. Ginidi received the B.Sc. degree in electrical engineering from Fayoum University, Fayoum, Egypt, in 2007, and the M.Sc. and Ph.D. degrees from Cairo University, Cairo, Egypt, in 2010 and 2015, respectively. He is currently an Associate Professor with Suez University, Suez, Egypt. His main research interests include operation, control, and planning of power system, application of optimization algorithm in power system, renewable integration, and smart grid.

Abdullah M. Shaheen received the B.Sc. degree from Suez Canal University, Port Said, Egypt, in 2007, and the M.Sc. and Ph.D. degrees from Menoufia University, Shebeen EI Kom, Egypt, in 2012 and 2016, respectively. He is currently with the Department of Electrical Engineering, Faculty of Engineering, Suez University, Suez, Egypt. His research interests include operation, control, and planning of power system, application of optimization algorithm in power system, renewable integration, and smart grid.